ARGONNE NATIONAL LABORATORY
9700 South Cass Avenue, Argonne, Illinois 60439

ANL–94/32

Distribution Category:
Thermal Science
(UC–1423)

Development of a Small-Channel Nucleate-Boiling Heat Transfer Correlation

by

K. E. Kasza and M. W. Wambsganss

Energy Technology Division

June 1994

Work supported by

U. S. DEPARTMENT OF ENERGY
Office of Energy Efficiency and Renewable Energy

DISCLAIMER

DISCLAIMER

Portions of this document may be illegible in electronic image products. Images are produced from the best available original document.

Contents

Figures

Tables

Nomenclature

A	Heated surface area
a(t)	Vapor bubble radius during growth at heated wall; Eq. 10
b	Empirical constant accounting for asphericity of growing bubbles; Eq. 12
C_p	Specific heat
C_s	Coefficient reflecting influence of wall on bubble diameter; Eq. 11
C_q	Proportionality coefficient in Eq. 4
C_{sf}	Proportionality coefficient in Eq. 15
D_b	Vapor bubble diameter at departure from heated surface
f	Frequency of vapor bubble formation
F	Function used to relate correlation parameters
g	Acceleration of gravity
G_b	Mass velocity of vapor bubbles leaving heated surface
h	Heat transfer coefficient of wall
h_{fg}	Latent heat of vaporization
Ja	Nondimensional Jakob number
K	Proportionality coefficient in bubble growth rate model; Eq. 10
k	Thermal conductivity
L_s	Length scale ratio of vapor bubble diameter to size of channel cross section
n	Exponent on time in bubble growth rate model; Eq. 10
N	Number of points of vapor bubble nucleation per unit area of heated surface
Nu	Nondimensional Nusselt number based on vapor bubble diameter
n_1	Exponent of bubble Reynolds number in correlation; Eq. 15
n_2	Exponent of Prandtl number in correlation; Eq. 15
Pr	Nondimensional Prandtl number
q	Heat input at wall
q/A	Heat transfer by vapor bubbles per unit heated wall area
Re_b	Nondimensional Reynolds number based on vapor bubble diameter

Re_{ch} Nondimensional Reynolds number based on channel hydraulic diameter

t Time during bubble nucleation process

T_w Temperature of wall

T_{sat} Saturation temperature of fluid

β Vapor bubble contact angle at wall

η Fluid thermal diffusivity; Eq. 12

μ Viscosity

ρ Density

σ Surface tension

Subscripts

ℓ Liquid property

v Vapor property

Development of a Small-Channel Nucleate-Boiling Heat Transfer Correlation

by

K. E. Kasza and M. W. Wambsganss

Abstract

Development of an improved semimechanistic-based set of correlation parameters for nucleation-dominant flow-boiling heat transfer in small channels is described. Formulation of these parameters is on the basis of a recently published open-literature model for vapor bubble growth at a heated surface. This work is part of a program directed at obtaining an understanding of the physical mechanisms that influence boiling in compact heat exchangers through the use of high-speed video and microscope optics to characterize bubble nucleation, growth, and interaction with the confining walls of small heat transfer passages. The correlation parameters presented here represent the first step in the development of an improved boiling correlation for geometrically confined small-channel flows. In such flows, the nucleating bubbles can become nominally the same size as the channel cross section, thereby invalidating existing correlations that are based on large-channel data. Initial efforts to correlate small-channel-boiling data obtained at Argonne National Laboratory from nontransparent electrically heated metal tube tests appear promising.

1 Introduction

This report describes the first stage in the development of an improved semimechanistic-based set of heat transfer correlation parameters for nucleation-dominant flow-boiling in small channels. Formulation of these parameters is based on a model (recently published in the open literature) for vapor bubble growth at a heated surface. This work is part of a program directed at obtaining a better understanding of the physical mechanisms that influence boiling in compact heat exchangers through utilization of high-speed video and microscope optics to characterize bubble nucleation, growth, and interaction with the confining walls of small heat transfer passages. The correlation parameters presented here represent the first step in the development of an improved boiling correlation for geometrically confined small-channel flows. In such flows, the nucleating bubbles can become nominally the same size as the channel cross section, thereby invalidating existing correlations that are based on large-channel data. Initial efforts to correlate small-channel refrigerant boiling data obtained at Argonne National Laboratory (ANL)

from nontransparent electrically heated metal tube tests appear promising. Also described is a newly completed boiling-flow-visualization test apparatus that utilizes ultra-high-speed digitized video and high-magnification microscope optics to study small-channel boiling phenomena.

Certain physical mechanisms that influence boiling become important as heat transfer channels become smaller; these mechanisms are not important in large channels. Results from an ANL scoping assessment of mechanisms that are potentially important in small-channel boiling will be presented in a companion report (Kasza and Wambsganss 1994). The mechanisms that will be highlighted in the companion report have been largely ignored in the development of currently used heat transfer correlations. The current correlations are mainly derived from data obtained from channels that are larger than those found in compact heat exchangers. When these mechanisms are more fully understood, criteria can be developed for defining when a channel is "large" and when it should be characterized as "small." Small-channel boiling tests have shown that boiling behaves differently in small channels than in large channels (Wambsganss et al. 1993; Tran et al. 1993); in particular, a nucleate boiling mechanism is shown to dominate to low values of wall superheat. Understanding these mechanisms will ultimately result in improved models and correlations for predicting boiling heat transfer in compact heat exchangers.

1.1 Compact Heat Exchangers and the Process Industries

The process industries, which convert raw materials into products, are very energy-intensive; in 1990, these industries used ≈23 quads, or about two-thirds of the energy consumed by all U.S. industries. Consequently, the potential for energy savings by improving the efficiency of the thermodynamic processes involved, or via more efficient heat exchange processes, is significant.

Two-phase flows and phase-change heat transfer are frequently encountered in process plants. Two-phase flow and heat transfer in circular channels of moderate to large size have been studied in depth over the past four decades. However, two-phase flow and heat transfer in small noncircular channels have received very little attention; even small circular channels have not been adequately studied. Nevertheless, small channels, especially those with noncircular cross sections, have taken on new importance in recent years, because of trends to (1) improve process plant performance and efficiency through the use of advanced heat exchange technology (Shah and Robertson 1993), and (2) reduce the size of plant equipment as in "process intensification," which is a strategy to reduce the size of a process plant to achieve a given production objective (Shah 1991).

In general, compact heat exchangers exhibit high thermal effectiveness, small size, low weight, pure counterflow operation, design flexibility, and the ability to handle multiple streams. High-performance heat exchangers, which feature small noncircular channels and include laminar and microchannel heat exchangers, can achieve surface area density ratios >3,000 m^2/m^3 and volumetric heat transfer coefficients as high as 7 MW/m^3K (equivalent values for shell-and-tube and plate heat exchangers are 0.21 and 1.25 MW/m^3K, respectively).

Today, there is worldwide interest in compact heat exchangers of the plate-fin, laminar, and microchannel types (Shah 1991; Wambsganss and Shah 1994). Advanced manufacturing methods and materials, as highlighted by Reay (1988), have surpassed our ability to design an optimal heat transfer surface for a given heat duty. For example, designers may know from trial and error that a particular tube channel geometry and size improves boiling heat transfer, but in general, they do not understand the basic mechanisms involved and therefore are unable to optimize their designs or extrapolate with confidence to a hybrid design. Research that addresses the fundamental issues associated with multiphase flow and heat transfer in small channels is needed. The ongoing work described in this report directly addresses this need.

1.2 Current Status of Understanding

For a given heat exchanger type, it is especially important to identify and understand the various heat transfer mechanisms that may be operable and the parameter ranges over which they are dominant. This importance stems from the fact that the analyst must know and understand the heat transfer mechanisms to appropriately model and correlate the heat transfer data, whereas the designer must know the dominant mechanism to appropriately apply the design correlations available to him.

The following is a brief summary of some of the pertinent findings from experiments on small, electrically heated, nontransparent, metal channels with boiling refrigerants. Findings reported by Wambsganss et al. (1993) and Tran et al. (1993) support the conclusion that for the range of parameters tested, a nucleate-boiling mechanism dominates heat transfer in small rectangular and circular channels (channels 3 mm or smaller in cross section) for vapor qualities to as large as 0.8. In contrast, for large channels, it is generally accepted that nucleate boiling does not exist at vapor qualities much above 0.2. The heat transfer coefficient for small-channel vaporization is shown to be dependent on heat flux and independent of mass flux and quality under a wide range of conditions. For tests performed at a constant saturation temperature, the data can be correlated approximately by a straight line on a log-log plot of wall heat flux q/A versus wall superheat $T_w - T_{sat}$.

For fully developed nucleate boiling, a decrease in saturation pressure shifts the boiling curve to the right and an increase in saturation pressure shifts the curve to the left. Typical refrigerant R-12 boiling data for a small round 2.46-mm-dia. brass channel at two vapor pressures is shown in Fig. 1. The data corresponding to a saturation pressure of 0.52 MPa, compared with that for a pressure of 0.82 MPa, are indeed shifted to the right, a finding that supports the dominance of a nucleation mechanism.

The test results of Tran et al. (1993) show that a nucleation mechanism dominates down to wall superheats as low as 3°C, and possibly even lower. However, other researchers of vaporization in compact heat exchangers, such as Robertson (1979); Robertson (1983); Robertson and Wadekar (1988); Wadekar (1992); and Carey and Mandrusiak (1986), concluded that convective boiling is the dominant heat transfer mechanism, and that nucleation does not contribute.

Hence, the results from various investigations have led to differing, and sometimes conflicting, conclusions relative to the dominant heat transfer mechanism(s) for vaporization in compact heat exchangers. Despite these

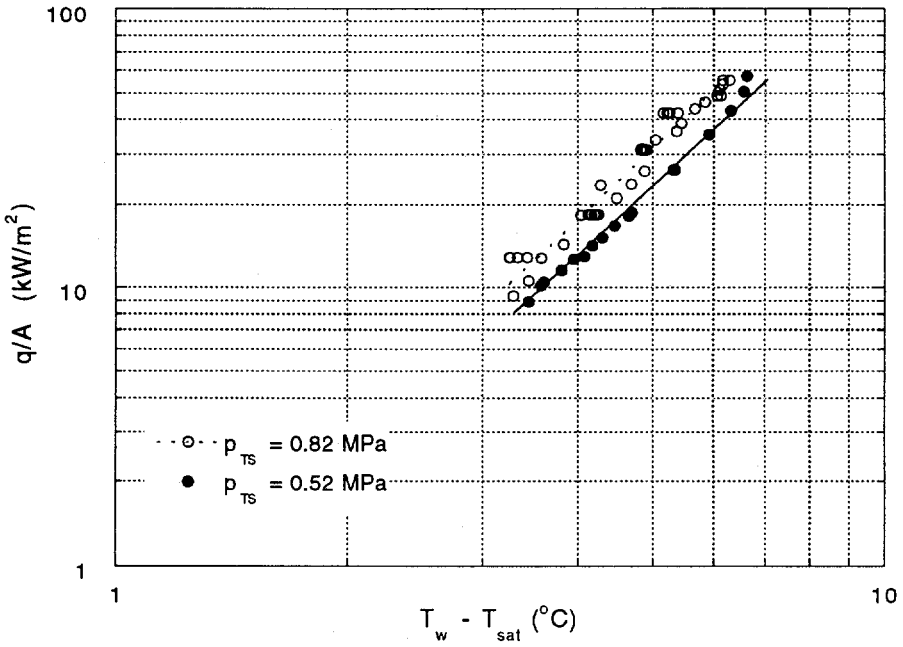

Fig. 1. Plot of wall heat flux q/A versus wall superheat $T_w - T_{sat}$ for refrigerant R-12 boiling in round brass 2.46-mm-dia. electrically heated channel exhibiting nucleate boiling at two pressures

differences, it is essential that ultimately "all of the pieces fit together" to form one coherent "flow-boiling scenario" for small channels. To this end, it is instructive to review the situation for flow boiling in large tubes. Steiner and Taborek (1992), as well as other investigators, have used the boiling curve (a plot of wall heat flux versus wall superheat) as a tool to distinguish between the two dominant mechanisms of flow boiling, viz., convective boiling and nucleate boiling. On the boiling curve illustrated in Fig. 2, two distinct regions can be identified with a transition region between them: Region A is a convective-boiling region; Region C is a fully developed nucleate-boiling region; and Region B is a transition region.

The characteristics of the two fundamental boiling-heat transfer mechanisms are quite different. In the convective-boiling region (A), the heat transfer coefficient is dependent on mass flux and quality, and independent of heat flux. Therefore, for

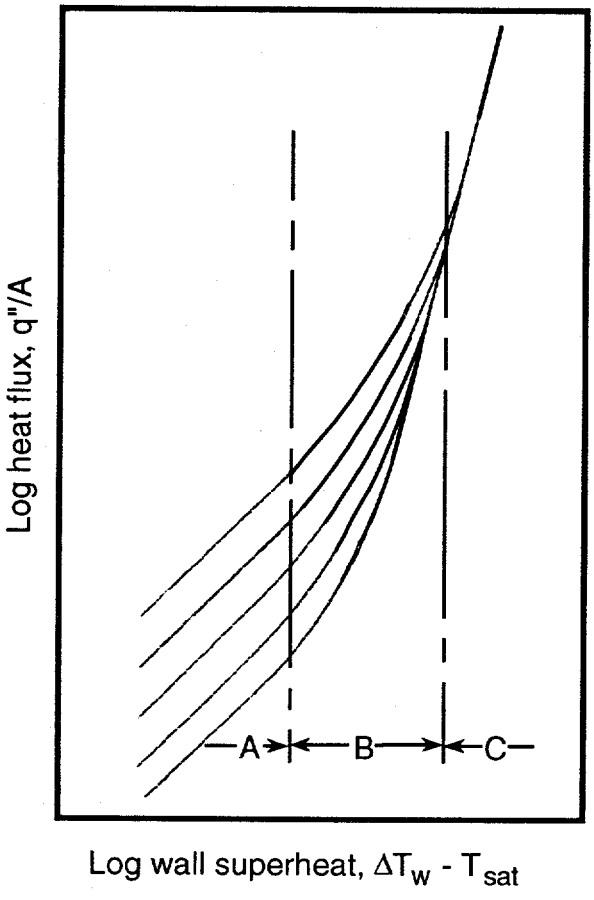

Fig. 2. Schematic representation of traditional boiling curve: Region A, convective boiling; Region B, transition; Region C, fully developed nucleate boiling

a given quality or mass flux, the resulting curves of heat flux versus wall superheat will be straight lines with slopes approximately equal to unity, as illustrated in Fig. 2. In the fully developed nucleate-boiling region (C), the heat transfer coefficient is dependent on heat flux, and essentially independent of mass flux and quality; as a consequence, the data will define a single curve, which can generally be approximated as a straight line with a slope greater than unity. (As noted above, in the nucleate-boiling region, pressure is also a parameter, and an increase in system pressure will cause this curve to shift to the left.) With regard to Transition Region B, Steiner and Taborek (1992) note that "The mechanism of the transition between the two regimes can be abrupt or more gradual, but it is not yet well understood; mass velocity, dissolved gases, and especially the distribution of the nucleation cavity sizes play a significant role."

Additional ANL flow-boiling test data for R-12 in a circular brass tube, performed at two distinct values of mass flux (75 and 150 kg/m^2s), at low superheats, are shown in Fig. 3. The data exhibit what is traditionally described as a convective-boiling region and the onset, rather abruptly at 3°C, of a fully developed nucleate-boiling region.

If the transition wall superheat is taken to be a function of the fluid and the channel (geometry, size, and surface condition), the boiling curve can be used to reconcile the differences in the conclusions arrived at by the various investigators relative to the heat transfer mechanisms. In particular, it appears that one effect of a reduction in channel size may be reduction in the value of the critical wall superheat associated with the transition to fully developed nucleate boiling. Peng and Wang (1993) supported this general observation when they concluded that nucleate boiling is greatly intensified in a small channel and that the wall superheat for flow boiling in a small channel may be much lower than that for larger channels for the same wall heat flux.

Kedzierski and Kaul (1993) have investigated boiling in mixtures of refrigerants and mixtures of refrigerants and lubricants for tubes of ≈9 mm in size. They found nucleate boiling over only a narrow range of conditions and made the statement that nucleate boiling in most direct-expansion evaporators occupies only a small fraction of the heat exchange area, with most of the area being in the convection regime. Based on the ANL data, it appears that this statement may only be true for the larger-sized tubes explored by Kedzierski and Kaul (1993), and not for the smaller tubes common to compact evaporators.

Kedzierski and Kaul (1993) also studied the narrow nucleate-boiling regime in the larger tubes by flow visualization and found for R-134a and R-134a plus an ester lubricant, bubble sizes on the order of 0.3 mm in dia. and that the presence of

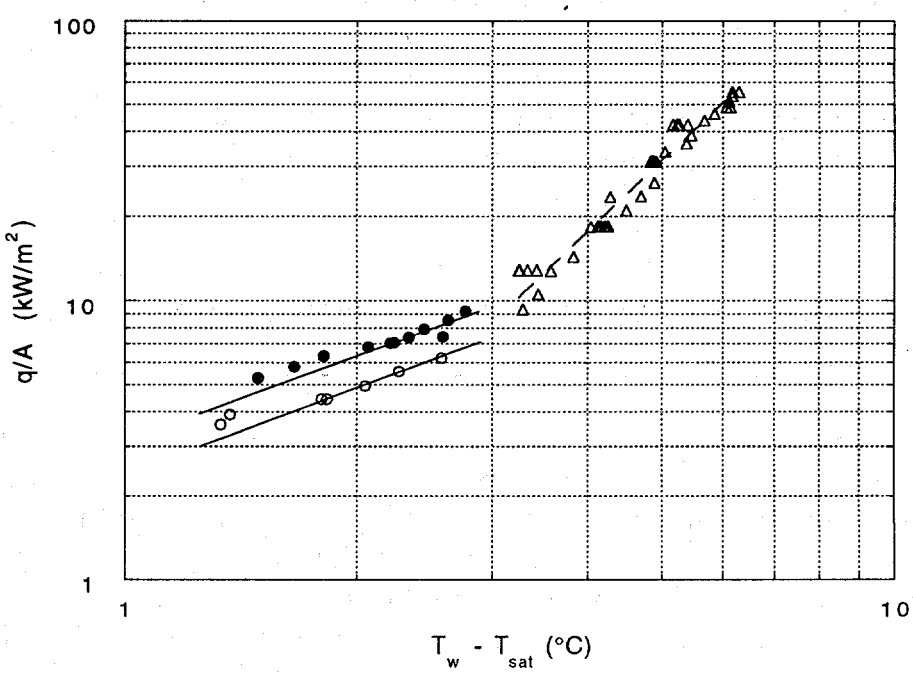

Fig. 3. Plot of wall heat flux q/A versus wall superheat $T_w - T_{sat}$ for refrigerant R-12 boiling in round brass 2.46-mm-dia. electrically heated channel exhibiting boiling at nominal pressure of 0.82 MPa for two mass fluxes at small superheats; o - G = 75 kg/m^{2}s; ● - G = 150 kg/m^{2}s; -▲- - nucleate boiling

a lubricant can have a strong and unpredictable influence on bubble size. They also stated that for large channels, there are no satisfactory, generally applicable heat transfer correlations for nucleate-flow boiling when lubricants are present.

Hence, nucleate boiling, because of its prevalence over a wide range of conditions, takes on added importance in understanding boiling in small channels and in developing improved heat transfer correlations. Furthermore, no generalized validated correlations have been formulated that account for geometrical-confinement effects that are imposed by the small channels associated with compact evaporators on vapor bubble formation. Researchers at ANL are performing scoping studies directed at delineating various mechanisms that influence boiling in small channels. The findings from these scoping studies, to be reported by Kasza and Wambsganss (1994) in a companion report, show that for a wide range of conditions, nucleation-generated bubbles can be of the same nominal size as the channel flow cross section in compact evaporators and that as a a result the multiphase flow regimes are drastically different in small channels due to vapor bubble confinement

and bubble interactions; therefore, heat transfer behavior in small channels differs considerably from that occurring in large channels.

The following sections describe the steps taken toward developing an improved heat transfer correlation for small channels in which nucleate boiling predominates. The approach taken is semimechanistic.

2 Semimechanistic Approach to Development of Correlations

Nucleated vapor bubbles can be nominally the same size as the channel cross section in compact evaporators. Therefore, there should be a characteristic length-scale parameter in the correlations that is a measure of the relative size of the bubbles and channel, at least to the extent of defining a threshold condition to establish when additional phenomena are important (i.e., quantifying at least when a channel should be called "large" or "small," and when a correlation formulated from large-channel data is no longer valid for small channels). Ultimately the parameter would appear explicitly in a robust heat transfer correlation of wide applicability that reflects the importance of the various phenomena that occur in both large and small channels.

The approach taken by Rohsenow (1952) to develop his correlation for nucleate-pool-boiling heat transfer, and the many derivatives of it (including extensions of it to flow boiling in channels by inclusion of an additional convective term) draw on mechanistic insights into various phenomena. Even though incomplete, the approach highlights various relevant nondimensional modeling parameters and then correlates the parameters experimentally. These approaches have produced correlations that do not have a vapor bubble diameter or a characteristic channel cross-sectional dimension appearing explicitly in them as size-scaling parameters. In addition, these correlations are based on simplified nucleate vapor bubble growth and behavior models obtained from experiments for unconfined pool boiling. In these experiments, the fluid reservoir that contains the fluid is large relative to bubble size; hence, geometrical confinement effects are negligible. Furthermore, there is no forced component of flow. The only gross fluid motion is due to induced stirring, which may be quite vigorous in some cases, produced by nucleate vapor bubbles generated at a heated wall.

The classical approach used by Rohsenow (1952) to develop his semimechanistic-based, nondimensional correlation parameters for unconfined nucleate-pool boiling is based on a simplified model of bubble growth and wall departure bubble size. An evaluation of Rohsenow's approach has led to an improved initial set of correlation parameters for nucleate boiling. This has been

accomplished in a manner analogous to that followed by Rohsenow, but using the latest improved mechanistic model of nucleating-bubble growth and bubble departure diameter developed recently by Zeng et al. (1993) for geometrically unconfined flows with a forced flow velocity.

Rohsenow's early work (1952) and that of many of his predecessors use the bubble model of Firtz (1935). This model, based on a balance between bubble surface tension and buoyancy forces, predicts vapor bubble diameter at departure from a wall in unconfined nucleate-pool boiling. Zeng et al. (1993) showed that bubble departure may be more correctly governed by a balance between dynamic bubble growth forces and buoyancy forces rather than a balance between surface tension and buoyancy forces. Utilizing the new mechanistic understanding developed by Zeng et al. (1993) for bubble behavior shows promise of ultimately yielding nondimensional correlation parameters for nucleate-boiling heat transfer in convective flows. The actual bubble characteristics and wall departure diameter are allowed to change with the magnitude of the flow velocity, thereby including some effects of convective bulk flow on nucleate boiling. This improves and broadens the applicability of the resulting correlation.

The parameters presented at this stage, however, still do not account for geometric confinement effects. Achieving this next step is one of the primary remaining goals of this program and is the reason for the boiling-flow-visualization experiments described in Sec. 4.

The parameters presented in this report are a bubble-size-based Reynolds number, a ratio of the liquid-superheat-enthalpy-at-the-wall to the latent-enthalpy-of-vaporization, and a liquid Prandtl number. Their correctness will continue to be evaluated in the remaining phases of this program. Using data from the ANL flow-visualization studies, we will further improve the bubble models and correlation parameters to include the confining effects of the small channel cross section on bubble growth characteristics. This will lead to an improved understanding of boiling heat transfer and robust practical correlations. Derivation of the modeling parameters is presented next. First, the Rohsenow (1952) approach is outlined and then its extension to incorporate the new bubble behavior model of Zeng et al. (1993) is given.

2.1 Classical Approach

The two-phase heat transfer Nusselt number (Nu) can be expressed as a function of nondimensional parameter groupings as

$$Nu = F(Re_{ch}, Re_b, Pr, L_s) \quad (1)$$

where Re_{ch}, the channel Reynolds number, is based on hydraulic diameter; Re_b, the bubble Reynolds number, is based on vapor bubble size at departure from a wall; Pr is the liquid Prandtl number; and L_s is a measure of length scale and reflects relative size of bubbles and channel cross section. The unknown function F can be determined completely experimentally or from experimental data and knowledge obtained from simplified mechanistic models.

The two Reynolds numbers Re_{ch} and Re_b are measures of the heat-transfer-promoting mixing produced by fluid turbulence and bubble growth, respectively. Recent boiling flow visualization data from ANL shows bubble growth mixing is highly intensified in small channels. The bubble-based Reynolds number was introduced by Rohsenow (1952) into the correlation he developed for unconfined nucleate-pool boiling. The length scale L_s is introduced in an attempt to account for the influences of geometric confinement on bubble behavior. This influence is the result of the very large size of the vapor bubbles, relative to the channel size in compact heat exchangers; it could be defined as the ratio of bubble size D_b, to be defined later, and the dimension of the channel cross section.

Even though the nondimensional parameters are shown as independent variables in Eq. 1, it is possible that a functional relationship exists between some of them under certain conditions. For example, some portion of the size-scaling effects may be accounted for by the parameter Re_b through bubble-size dependence on channel dimensions as a result of geometric confinement. These relationships will be clarified when sufficient information is developed to establish how nucleating bubbles in a geometrically confined space differ in size from those that develop in large unconfined fluid regions, which is the only case for which the existing bubble models are valid. A similar dependence may exist between the two Reynolds numbers as a result of possible dependence of nucleating-bubble size on the mean fluid velocity of the channel.

As background, attention will be focused first on the heat transfer of unconfined nucleate-pool boiling, which is the case addressed by Rohsenow (1952). For this case, Eq. 1 reduces to

$$Nu = F(Re_b, Pr). \quad (2)$$

The channel Reynolds number Re_{ch} has been eliminated because no forced fluid motion is present, other than that caused by local agitation of the fluid at the heated surface by the growing and departing vapor bubbles. Nevertheless, in fluid volumes that are large relative to the size of individual bubbles, rising bubbles can often cause vigorous large-scale convection currents that can influence the hot

thermal layers at a heated surface and alter nucleation characteristics. L_S is eliminated because it is assumed that the bounding geometry does not influence bubble nucleation or convection currents. This matter is being explored more thoroughly with boiling-flow visualization studies on small, heated, glass rectangular cells, as highlighted in Sec. 4.

Rohsenow (1952), using the best mechanistic bubble model available in the literature at that time, defined the bubble Reynolds number as $Re_b = G_b D_b/\mu_\ell$, where G_b is the mass velocity of the bubbles as they leave the heated surface, D_b is the bubble diameter as it leaves the heated surface, and μ_ℓ is the liquid viscosity. G_b can be written as

$$G_b = \frac{\pi}{6} D_b^3 f \rho_v N, \tag{3}$$

where f is the frequency of bubble formation, ρ_v is the density of saturated vapor, and N is the number of nucleation sites per unit area of heated surface.

Drawing on the work of Jakob (1949), Rohsenow (1952) used the facts that the product of f and D_b is approximately a constant and that the number of nucleation sites is nearly proportional to the surface heat flux for a given pressure. These facts allowed him to relate heat transfer by the bubbles per unit area q/A to the heat transfer associated with a single site. This relationship is defined by the equation

$$\frac{q}{A} = C_q h_{fg} \rho_v N \frac{\pi}{6} D_b^3 f, \tag{4}$$

where the coefficient C_q may be a function of pressure and h_{fg} is the latent heat of vaporization. Substituting Eqs. 3 and 4 into the expression for Re_b yields

$$Re_b = \frac{1}{C_q} \frac{D_b \left(\frac{q}{A}\right)}{\mu_\ell h_{fg}}, \tag{5}$$

where, importantly, the term f N is factored out.

At this point we have a set of three nondimensional parameters, given by

$$Re_b = \frac{1}{C_q}\frac{D_b\left(\frac{q}{A}\right)}{\mu_\ell h_{fg}},$$

$$Nu = \frac{hD_b}{k_\ell}, \tag{6}$$

and

$$Pr = C_{p\ell}\mu_\ell / k_\ell,$$

where $h = (q/A)[1/(T_w - T_{sat})]$ is the heat transfer coefficient of the heated surface film, $(T_w - T_{sat})$ is the difference between the local wall temperature and the saturation temperature of the fluid, and k_ℓ is the thermal conductivity under saturation conditions (the subscript ℓ denotes liquid properties under saturation conditions).

If these parameters are to be of practical use, the bubble diameter D_b must be expressed in terms of easily quantifiable parameters, even though it could be measured experimentally on a case-by-case basis in the absence of reliable mechanistic models. Rohsenow (1952) used the Firtz (1935) model, which is given by

$$D_b = 0.0204\beta\sqrt{\frac{\sigma}{g(\rho_\ell - \rho_v)}}, \tag{7}$$

where β is the bubble contact angle at the wall, σ is the surface tension of the liquid-vapor interface, ρ_ℓ is the density of the saturated liquid, ρ_v is the density of the vapor, and g is the acceleration of gravity. Equation 7 can then be substituted into Eqs. 6.

Another equivalent nondimensional parameter can be defined as

$$\frac{C_{p\ell}(T_w - T_{sat})}{h_{fg}} = Re_b\, Pr/\, Nu\,. \tag{8}$$

This is allowed because the theory of dimensional analysis permits us to combine a group of nondimensional parameters to form a new parameter. This allows q/A to be eliminated from one of the nondimensional parameters and we are left with the correlation developed by Rohsenow (1952) i.e.,

$$\frac{C_{p\ell}(T_w - T_{sat})}{h_{fg}} = C_{sf}\left[\frac{q/A}{\mu_\ell h_{fg}}\sqrt{\frac{\sigma}{g(\rho_\ell - \rho_v)}}\right]^{0.33} Pr^{1.7}. \quad (9)$$

Many sets of experimental data were used by Rohsenow (1952) to establish the functional relationship between the three parameters (i.e., to establish the exponents on the nondimensional parameters and the value of C_{sf}). The new parameter, given by Eq. 8, replaces Nu in Eqs. 6 and represents the ratio of liquid superheat enthalpy at the heated surface to the latent enthalpy of evaporation. The coefficient C_{sf} is a strong function of surface/fluid combinations and surface finish; also embedded in it is the quantity β and possibly some dependence on pressure. Rohsenow (1952) presents some values of C_{sf} for various fluid/surface combinations. However, C_{sf} can also be a function of subtle differences in surface finish and small amounts of liquid or surface contaminants. For a brass/water interface combination, Rohsenow (1952) reports $C_{sf} = 0.0060$. Vachon et al. (1968) also report values of C_{sf} for additional fluid/surface combinations and state that the exponent on Pr can vary from 0.8 to 2.0, depending on surface cleanliness.

The attractiveness of this correlation is that only one set of experimental values for q/A and $T_w - T_{sat}$ is necessary to determine the coefficient C_{sf} for a given fluid/surface combination. The correlation can be used for a wide range of thermal conditions for the same fluid/surface combination. This type of expression has seen considerable application and, with some modifications, has been applied to forced confined-boiling flows where the heat transfer is modeled as the sum of a convective and nucleate boiling contribution. It should be noted that this correlation was developed for unconfined nucleate-pool boiling without forced flow. The correlation includes bubble size but contains no explicit parameter for channel size and hence no relative measure of bubble and channel size that would allow delineation of a small versus large channel. Nevertheless, it has been applied in modified forms to confined forced flows in large channels with reasonable success.

2.2 Correlation Based on Improved Nucleate-Bubble-Growth Model, and Some of Its Features

The very recent mechanistic model of Zeng et al. (1993) for predicting D_b will be introduced into the nondimensional parameters given by Eqs. 6 and 8. Zeng et al. (1993) developed a model for the motion of a nucleating bubble on an upward-facing heated horizontal surface based on the forces they determined to be important. Their initial work for pool boiling was extended to account for forced flow parallel to a heated surface without any other wall confinement.

The model for bubble liftoff assumes a balance between unsteady dynamic-bubble-growth forces and bubble buoyancy. This is in contrast to most other models, such as that of Firtz (1935), which assume a balance between surface tension and buoyancy at liftoff. The model of Zeng et al. (1993) does not include the often difficult-to-quantify surface tension or bubble contact angle. It uses a generally accepted vapor bubble growth rate model of the form

$$a(t) = Kt^n, \tag{10}$$

where a(t) is the bubble radius, t is time in the growth process, and K and n are experimentally determined. Equation 10 is used in dynamic force balance equations to evaluate the unsteady growth forces acting on a growing vapor bubble.

The expression given by Zeng et al. (1993) for liftoff bubble diameter is

$$D_b = 2\left\{\frac{3}{4}\frac{K^{\frac{2}{n}}}{g}\left[\frac{3}{2}C_s n^2 + n(n-1)\right]\right\}^{\frac{n}{(2-n)}}, \tag{11}$$

where C_s is a coefficient reflecting the influence of the wall on the bubble. The value of C_s has been determined empirically, with only a very limited data base, to be equal to 20/3. Although this value is used here, its correctness will be explored this program.

At this stage in the correlation development, one could perform experiments for the specific fluid/surface combination of interest to determine the values for K and n in Eq. 10 and then use these values in Eq. 11. However, we will use Zuber's (1961) mechanistic diffusion-controlled bubble-growth model,

$$a(t) = \frac{2b}{\sqrt{\pi}} Ja\sqrt{\eta(t)}, \tag{12}$$

where

$$Ja = \frac{\rho_\ell C_{p\ell}(T_w - T_{sat})}{\rho_v h_{fg}}, \quad \eta = \frac{k_\ell}{\rho_\ell C_{p\ell}},$$

and b is an empirical constant that accounts for asphericity of a growing bubble. A value of b = 0.5 was obtained by Zeng et al. (1993) from limited water data. Ja is nondimensional and is called the Jakob number, and η is fluid thermal diffusivity.

This model has been found most useful for near- and subatmospheric pressure conditions.

A comparison of Eqs. 10 and 12 yields expressions for n and K, which are then substituted into Eq. 11 to yield the following expression for bubble liftoff diameter

$$D_b = \frac{3}{2^{\frac{1}{3}}}\left(\frac{2b}{\sqrt{\pi}}\right)^{\frac{4}{3}} Ja^{\frac{4}{3}}\left(\frac{\eta^2}{g}\right)^{\frac{1}{3}}. \qquad (13)$$

The term $(\eta^2 / g)^{1/3}$ has dimensions of length and physically is a measure of the thickness of the fluid thermal layer at the heated surface. Griffith (1958) has shown that a growing vapor bubble is influenced by whether it is fully submerged or extends beyond the wall thermal layer during its growth. The value of D_b can be nondimensionalized with this thermal-layer thickness.

These features are not present in the Firtz (1935) model for D_b, i.e., Eq. 7. Furthermore, σ and β are absent and D_b is a strong function of wall superheat in this new model. In this nondimensionalized form, bubble lift-off diameter is only a function of Ja and b. Based on the new model, D_b decreases with increasing pressure because Ja decreases with increasing pressure because vapor density ρ_v depends on pressure. D_b also increases with wall superheat, $(T_w - T_{sat})$, a finding that agrees with some preliminary experimental observations of Kasza and Wambsganss (1994). In contrast, Firtz's (1993) model, which is based on surface tension forces, is not a function of wall superheat, but is a function of pressure.

To give some quantitative appreciation of Eq. 13, it was evaluated for water and the results are compared with those predicted by the Firtz (1993) model given by Eq. 7. The conditions chosen for the comparison are atmospheric pressure, $(T_w - T_{sat}) = 8°C$, $T_{sat} = 100°C$, and b = 0.86, a value used by Zeng et al. (1993) for conditions similar to these. For these conditions, Ja = 31.16 and $(\eta^2 / g)^{1/3} = 0.0142$ mm, yielding $D_b = 3.19$ mm. This value of D_b is close to the average size of 3.0 mm exhibited by limited-flow visualization data generated at ANL from nucleate-pool boiling with water in a large glass cell under similar conditions. Firtz's (1993) Eq. 7 with $\beta = 31°$ yields $D_b = 1.58$, which is considerably smaller than that based on the dynamic growth force model of Zeng et al. (1993), and smaller than that from the experimental (glass cell) data. The thermal-wall layer thickness, as represented by $(\eta^2 / g)^{1/3}$, is considerably less than the bubble diameter at wall departure and would also be considerably smaller than the ≈1-2-mm size of the small channels under study. Hence, the thermal-layer thickness is probably not a significant dimension unless the channels are very small or pressures are high enough to reduce bubble sizes significantly so that the bubbles are embedded more completely in the thermal layer.

The values of D_b predicted by the two models for refrigerant R-12 are shown in Table 1, along with the water values for comparison. This comparison shows that for the given conditions, nucleate-vapor bubbles in water can be larger than those in R-12. Hence, for a given channel size, the effects of channel geometric confinement would be potentially greater with water boiling than with R-12 boiling. However, it should be noted that, because of the influence of pressure on D_b, a considerably higher pressure in the water could reduce the bubble to a size smaller than that exhibited by R-12. Because the model of Zeng et al. (1993) (Eq. 13) employs the Zuber (1961) bubble growth model, which is most correct near atmospheric pressure, it should be used with reservations at elevated pressure.

The Zeng et al. (1993) model given by Eq. 11 is more general because it uses the growth rate model of Eq. 10 and presumably is not subject to the above-mentioned pressure limitations. However it requires specific experimental data on constants to be useful. In addition, the model of Zeng et al. (1993) only applies to unconfined regions; its validity will be evaluated under confined-boiling conditions by flow visualization in this program (see Sec. 4). In this regard, the presence of parameters b and C_s, which are used to account for bubble distortions and wall influence, hold some promise for being able to account for the effects of small-channel geometrical confinement. The range of validity of Eqs. 11 and 13 will be evaluated by testing progressively smaller channels and heated glass cells and using deterioration of their predictive capacity and change in visual bubble behavior as tools for defining when a channel is small.

Substitution of Eq. 13 into Eqs. 6 and 8 yields the following set of nondimensional modeling parameters, which are based on the improved mechanistic bubble dynamics model of Zeng et al. (1993):

Table 1. Predicted bubble diameter (mm) upon departure from a wall D_b, from Firtz (Eq. 7) and Zeng et al. (Eq. 13) for $(T_w - T_{sat}) = 8$°C, 0.1 MPa pressure: water and R-12

Source	Water	R-12
Firtz (1935) model	1.58	0.50
Zeng et al. (1993) model	3.19	0.37

$$Re_b = \frac{3}{2^{\frac{1}{3}}}\left(\frac{2b}{\sqrt{\pi}}\right)^{\frac{4}{3}} Ja^{\frac{4}{3}}\left(\frac{\eta^2}{g}\right)^{\frac{1}{3}} \frac{q/A}{\mu_\ell h_{fg}} \frac{1}{C_q},$$

$$Re_b\, Pr/\, Nu = C_{p\ell}(T_w - T_{sat})/\, h_{fg}, \tag{14}$$

and

$$Pr = C_{p\ell}\mu_\ell / k_\ell.$$

Based on experimental data, an empirical relationship for confined nucleate-flow boiling can be derived with these variables, just as Rohsenow (1952) did when he developed Eq. 9 for nucleate-pool boiling. This will be done in the experimental phase of this program with data obtained from glass-cell pool boiling and small-channel flow-boiling experiments with various fluids and geometries. This process will allow us to evaluate the validity and robustness of these correlation parameters.

This evaluation process will most likely highlight the need for one or more additional parameters to account for effects of channel geometrical confinement on nucleating-bubble behavior, as discussed earlier. The inclusion of new parameters will be carried out in building-block fashion to carefully justify the additional complexity and to establish ranges of validity for the various correlation subforms. Toward this goal, a brief look at some of the features of these correlation parameters is presented in the next section. Data from flow-boiling tests on refrigerants in an electrically heated, small, circular brass tube with an inside diameter of 2.46 mm will be used.

3 Preliminary Evaluation of Correlation with ANL Small-Channel-Boiling Data

It is instructive to assume that the nondimensional parameters in Eqs. 14 can be written as a function of the product of the parameters, each raised to some unknown exponent (this is a widely used and frequently valid assumption in developing empirical correlations in fluid mechanics and heat transfer), as given by

$$\frac{C_{p\ell}(T_w - T_{sat})}{h_{fg}} = C_{sf}\, Re_b{}^{n_1}\, Pr^{n_2}. \tag{15}$$

In this expression, n_1, n_2, and C_{sf} are determined with experimental data from carefully planned experiments and data analysis procedures. C_{sf}, as in the Rohsenow (1952) correlation (Eq. 9), is a function of the fluid/surface combinations and surface characteristics, such as roughness, which influence vapor bubble nucleation and growth behavior. With the substitution of Eqs. 14 into Eq. 15, it can be shown that the wall heat flux is related to the wall superheat by the equation

$$q/A \propto (T_w - T_{sat})^{\left(\frac{1}{n_1}-\frac{4}{3}\right)}. \tag{16}$$

This dimensional relationship contains the exponent n_1, but omits all other quantities, in particular fluid properties and C_{sf}. For a given fluid/surface combination and fluid properties that are not strong functions of temperature, and assuming that channel cross-sectional shape and size are not important, this dimensional relationship implies that the wall heat flux is a function of only the wall superheat raised to the power $(1/n_1 - 4/3)$. It is generally accepted that when experimental data on boiling exhibits this behavior, a nucleate-boiling mechanism dominates. This functional form is exhibited by ANL data under a wide range of conditions, as described earlier.

It is very informative to use some of the ANL refrigerant boiling data from heated metal channels to get a preliminary look at the value of n_1 and to compare this exponent with that appearing in the Rohsenow (1952) correlation, given by Eq. 9. For data on refrigerants R-12, R-113, and HFC-134a, and brass and stainless steel tubes of circular and rectangular cross section, the exponent of $T_w - T_{sat}$, based on experiment, seems to be in the range of 2.4-2.8, with the value being larger for round tubes (see Wambsganss et al., 1993; Tran et al. 1993). If we use an average value of 2.6, $n_1 = 0.25$. Hence, the exponent of Re_b in Eq. 15 is 0.25 as compared with 0.33 in the Rohsenow (1952) correlation. The similarity of exponents is reassuring in that both correlations reflect on nucleate boiling and Rohsenow's (1952) correlation has been successful for various types of data. Even though the exponents of Re_b in the two correlations are similar, the Reynolds numbers are defined fundamentally differently in terms of what forces govern nucleate-bubble wall departure and hence can exhibit differing degrees of proficiency in correlating various sets of data.

As discussed in Sec. 1.2, plots of wall heat flux q/A, versus wall superheat, $T_w - T_{sat}$, as represented in Fig. 2, were highlighted as fundamentally valuable in establishing whether boiling data is in the nucleate regime. To further explore the merits of the derived correlation parameters, data from ANL boiling tests in an electrically heated 2.46-mm-dia. circular metal channel for refrigerant R-12 is first presented in this standard plot form and then in terms of the nondimensional parameters Re_b versus $C_{p\ell}(T_w - T_{sat}) / h_{fg}$, as defined by Eq. 14.

The test apparatus and experimental procedures used to generate this data are described by Wambsganss et al. (1993). These tests were performed at two nearly constant pressure levels of 517 and 822 kPa, and covered a broad range of mass flux (63 to 832 kg/m^{2}s) and heat flux (2.53 to 59.5 kW/m^2); for the range of heat fluxes tested, wall superheat ranged from ≈0.67 to 6.63°C. All data are for a nearly constant Prandtl number ranging from ≈2.83 to 2.93. Hence, Pr is essentially constant for these tests, and its influence as one of the three important modeling parameters given by Eq. 14 will not be assessed here. Data for other fluids, and hence different Pr, will be used to assess the influence of this parameter in the future.

The plot of q/A versus $T_w - T_{sat}$, shown in Fig. 4, clearly shows two distinct regions of different slope with some data scatter in each region. The scatter in the region of steepest slope, the region of largest wall superheat, is the region for which data was taken at two pressure levels. The data for the lowest pressure fall below and to the right of those at the higher pressure. The scatter in the region of least slope is the region for which data were taken under conditions where they seem to exhibit, based on conventional thought, a dependence on mass flux or convective flow velocity. Based on classical wisdom applied to large channels, this region would be said to exhibit convective heat transfer characteristics, i.e., similar to Regions A or B in Fig. 2.

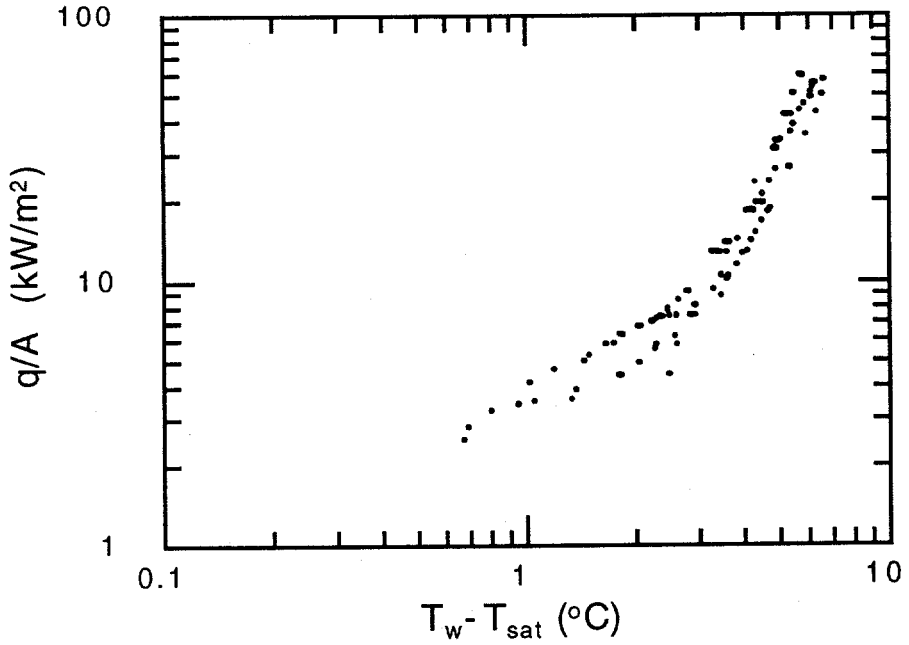

Fig. 4. Composite plot of boiling data in Figs. 1 and 3 for wall heat flux q/A versus wall superheat $T_w - T_{sat}$ for refrigerant R-12 in round brass 2.46-mm-dia. electrically heated channel at various pressures and mass fluxes

Figure 5 shows the same data plotted in terms of the proposed parameters. There is less scatter in both regions, with some scatter still present at intermediate values of both parameters. The vertical axis is the bubble Reynolds number Re_b, which is directly proportional to the product of bubble liftoff diameter D_b, and wall heat flux q/A (see Eqs. 6 and 14). The horizontal axis is directly proportional to the wall superheat $T_w - T_{sat}$ (see Eq. 14). As the value of Re_b increases, along with increasing wall superheat, the bubble diameter D_b can also increase. Hence, relative to the importance of geometric confinement effects, as discussed in Secs. 1.2 and 2.1, moving up along either region of the data curve can result in the bubbles becoming larger and hence their behavior being more strongly influenced by the channel. This implies that size scaling effects, or the parameter defined as L_s in Eq. 1, for an ultimate correlation would not only be a function of channel cross-section dimensions, but also of fluid type and thermal-hydraulic conditions. This implies that confinement effects can also grow or diminish with changes in quantities such as wall heat flux or pressure.

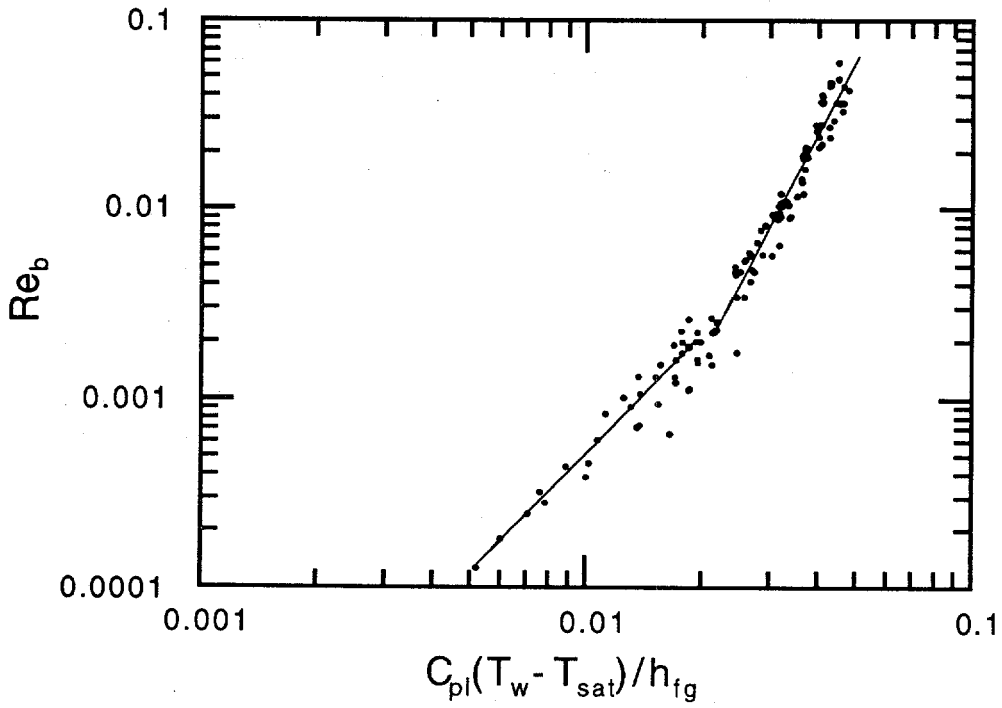

Fig. 5. Plot of boiling data in Fig. 4 in terms of nondimensional correlation parameters, bubble Reynolds number Re_b versus $C_{p\ell}(T_w - T_{sat})/h_{fg}$ for refrigerant R-12 in round brass 2.46-mm-dia. electrically heated channel at various pressures and mass fluxes

The data scatter in the steep-slope region is reduced because the influence of the two tested pressure levels is accounted for by pressure influence on bubble size. Bubble size strongly depends on vapor density and is contained in Re_b, as described in Sec. 2.2. These data are only for a narrow pressure range. Data for a wider range of pressures will be generated and used to further explore the influence of this parameter on the correlation.

Data scatter in the gentler-slope region is also reduced but not as cleanly. The behavior in this region will require more evaluation and study before a definitive explanation can be given. However, the discussion below describes some preliminary speculation on what may be happening in this region.

It appears that the correlation parameters may partially account for some of the influence of convective flow on heat transfer through the influence of bulk flow velocity on the wall temperature, which appears in the wall superheat term. This term appears in, and has a strong influence on, bubble size in the nucleate-bubble model (see Eq. 13) used to express the correlation parameter Re_b. Following this logic further, it is possible that this region of gentler slope is also a region of significant nucleate boiling. It can also be conjectured that the distinct change in slope between the two regions in Fig. 5 may be a result of an increasing importance of the influence of geometric confinement on bubble behavior with increasing values of Re_b and $C_{p\ell} (T_w - T_{sat}) / h_{fg}$. Thus, the region of gentler slope is typified by bubbles not large enough to be greatly influenced by the size of the channel cross section and they nucleate in a nearly classical fashion. (However, within the limits of conditions in which the contribution to total heat transfer is indeed dominated by convective rather than nucleate heat transfer, the influence of mass flux would have to be accounted for.) As we move upward along this curve, the bubbles become larger and start to reflect the confinement of the channel. The intermediate data scatter would suggest that a transition region exists where the bubble/bubble and bubble/wall interactions and flow patterns are unstable and intermittent and are about to undergo significant change. With a further increase in the influence of geometric confinement resulting from a further increase in bubble size, the bubbles become nominally the size of the channel, and take on the shape of the channel. An individual bubble, generated at a given nucleation site, cannot leave the wall but is confined to sweep or slide down the channel, coalescing with other nucleating bubbles and increasing the frequency of bubble generation on the heated walls. The sliding bubbles also cause thin-film nucleation in the thin liquid layer that exists between the moving bubble and the heated channel wall. The preceding has been confirmed in recent preliminary ANL flow visualization tests. Both of the preceding mechanisms can cause heat transfer to increase and help to explain the increased slope after the transition region is passed. As is apparent from the preceding discussion, flow visualization studies of bubble behavior in small heated channels will be very important to further improving our understanding of boiling under these conditions.

The next section describes ongoing efforts to improve our understanding of boiling in small channels through the use of flow visualization.

4 Direction of Future Investigations

As discussed above, boiling-refrigerant heat transfer data from small, electrically heated, nontransparent, metal channels show that heat transfer in channels ≈<3 mm in dia. differs considerably from that in larger channels. Also, several physical mechanisms that are potentially dominant in small channels but are of lesser importance in large channels have been identified. Very significantly, it has been shown that wall-boiling-generated vapor bubbles in several refrigerants and water, and probably in other liquids as well, can be nominally the same size as the channel cross-sectional dimensions in compact heat exchangers with channels of 3 mm or less. Hence, it is believed that bubble growth processes, together with bubble/bubble and bubble/channel wall interactions, can cause vigorous mixing and disruption of the confined channel flow and cause small-channel boiling to exhibit behavior that is different from that in large tubes. To study these mechanisms more thoroughly, a test apparatus employing extensive use of flow visualization has been built. Data from this apparatus, along with data from heated, all-metal nontransparent test sections will be used to further develop a mechanistic understanding of boiling in small channels, leading to improved heat transfer correlations.

The test apparatus has been designed to utilize state-of-the-art, ultra-high-speed, digitized, video-based flow visualization, and long-distance microscope optics to study the microscale/time-resolved behavior of boiling-generated vapor bubbles. Figure 6 is a schematic representation of the test apparatus, which is designed to be chemical- and corrosion-resistant to minimize fluid contamination and allow use of a variety of fluids of interest to industry. Most of the elements coming in contact with test liquids are made of Teflon, stainless steel, and other inert materials. The system is also capable of operating at elevated temperature and pressure. Various channel geometries can be tested.

Table 2 briefly describes the various components. The alphanumeric designators in the table correspond to labels in Fig. 6. The apparatus will initially be used with water. The test fluid is pumped in a closed loop through a heated transparent test section, with the fluid passing through a heat exchanger immersed in a constant-temperature bath to ensure a constant temperature at the test section inlet. The overall test fluid circuit is pressurized to a specified level with a pressurized accumulator tank. Pertinent temperatures, pressures, and flow rates are measured for use in data analysis, as well as for system control.

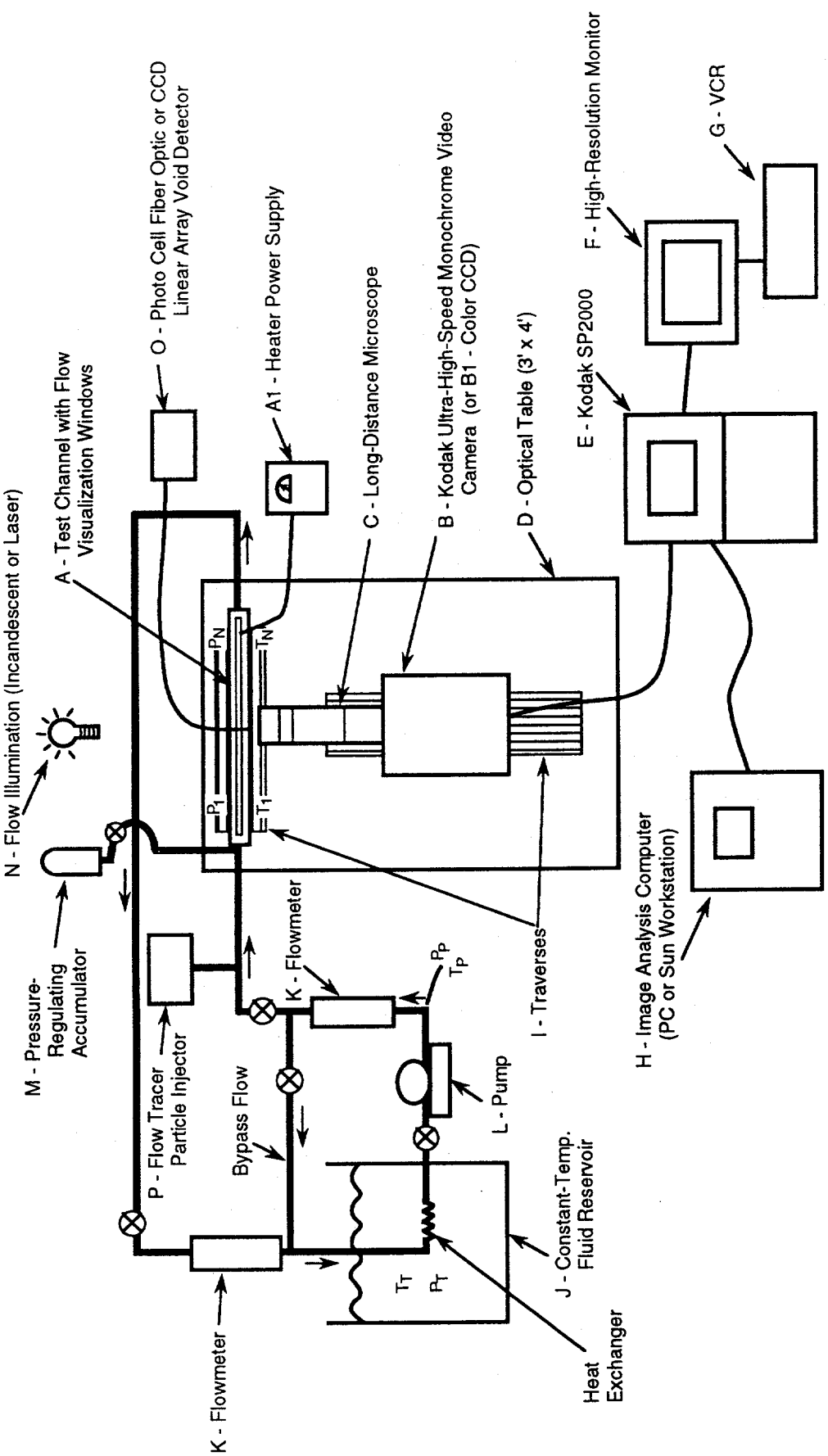

Fig. 6. Test apparatus for visualization of boiling flow in small channels

Table 2. Features of various components of flow-visualization test apparatus

A	Small channels, initially of rectangular cross section, with windows to allow viewing and illumination. Other geometries can be installed.
A1	One or more walls of the channel can be heated electrically with a DC power supply (for the initial rectangular channel, a short wall is heated and contains a few artificial nucleation sites at window locations).
B	High-speed Kodak monochrome CCD video camera capable of 60-2000 full video frames pps or 12000 part-frames pps will record motion and development of bubbles and interactions with each other and the confining channel walls, including the evolution of nucleating bubbles during heat transfer.
B1	High-resolution color CCD camera with fast electronic shutter to take high-resolution overall flow photos.
C	Long-distance microscope capable of micron-size resolution and depths of field comparable to size of channel cross section.
D	Optics table; supports camera, lens, and test channel to allow accurate spatial positioning and minimize relative vibrational motion.
E	Kodak SP2000 controls and video recorder/image digitizer analyzer.
F	High-resolution video monitor.
G	Standard video recorder for recording from color CCD camera and for converting SP2000 to standard format.
H	PC or Sun Workstation for processing of digitized video images to obtain bubble growth rates, void fractions, liquid transport velocity, etc.
I	Traversing mechanisms for positioning long-distance microscope/video camera.
J	Constant-temperature fluid reservoir for achieving and maintaining desired temperature at inlet to channel.
K	Flowmeters.
L	Low flow rate, high pressure, low-pulsation variable-speed pump to control flow into test channel.
M	Pressure-regulating accumulator for control of system pressure.
N	Flow illumination for video photography: either incandescent or argon laser.
O	Photo cell linear array, fiber-optic void detector for monitoring spatial variation of gas void across the channel.
P	Flow tracer micron particle injector for obtaining liquid velocity simultaneously with bubble behavior.
P_i	Pressure measurements.
T_i	Temperature measurements.

The test section, video camera, and microscope optics are mounted on a rigid 3 x 5-ft stainless steel optics bench to allow accurate, vibration-free viewing of the selected boiling field. The camera and optics are mounted on a 24-in. linear travel bed, allowing motion perpendicular to the test section, which along with several optical lenses, controls image magnification, field of view, and depth of field. The test section is mounted on a traversing bed that allows for observing boiling at various locations along the length of the heated channel.

The test section is designed to enhance the use of flow visualization. To achieve the very high video frame rates needed to study nucleate-vapor-bubble growth, high-intensity illumination with proper direction is required to avoid shadows in the field of view. Glass optical-cell boiling tests were used to develop and explore the flow visualization technique, establish essential features of the flow channel, and study bubble behavior in confined regions in the absence of forced flow. The glass cells are made of Pyrex and are open on one side. The bottom of a cell (the side opposite the opening) is placed in direct contact with an adjustable-temperature, electrically heated hot plate. The cell is filled with distilled water and open to the atmosphere. Three cell sizes are being tested. All are 50 mm tall and individually have the following regions of contact (i.e., heated areas) with the hot plate: 10 x 50 mm, 5 x 25 mm, and 1 x 25 mm; yielding gap sizes of 10, 5, and 1 mm between the parallel, glass viewing window walls of the cells. The rectangular-cross-section-channel geometry was chosen to begin the program because it typifies many plate-fin compact heat exchanger designs and replicates the all-metal channels that have undergone testing at ANL to establish boiling heat transfer coefficients.

The flow channel test section is shown in Fig. 7; it consists of three basic components. Two aluminum plates sandwich two window plates which, in turn, sandwich a Teflon flow channel sheet. A slot and circular flow plenum at each end of the slot are machined in the Teflon sheet. The slot and the two flow windows form the four sides of a rectangular channel in which boiling takes place. The boiling is produced by thin strip(s) of metal foil bonded to the edges of the Teflon slot. The strips are heated by dissipation of electrical current in the strips. One or both narrow sides of the channel can be heated. In addition, artificial nucleation sites, produced by needle point indentations or scratches on the foil, are used singly and in closely spaced groups to facilitate flow visualization of bubble behavior. The flow is observed and illuminated through the long sides of the channel by back lighting. Ports, bored in both window plates, are taped for Teflon pipe fittings. One set of ports each on the upstream and downstream ends of the channel are used to route the flow through the channel. The other two ports are used to route electrical and instrumentation leads into and out of the test section. Additional instrumentation, such as pressure taps and thermocouples, is located in small holes in the windows. By varying the thickness of the Teflon flow channel sheet and the

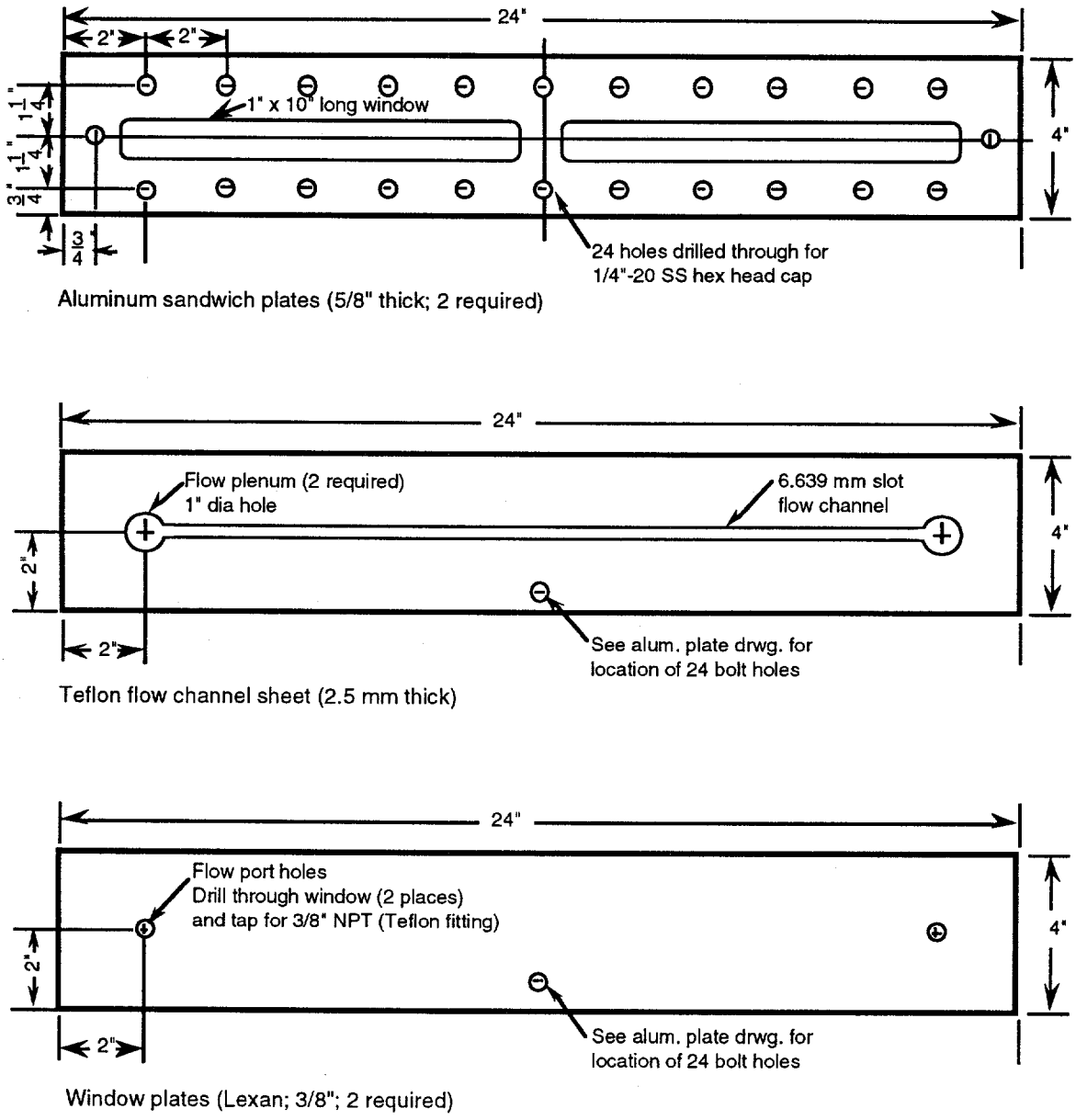

Fig. 7. Test section for visualization of boiling flow in a small rectangular channel

width of the machined slot, rectangular geometries of various dimensions can be tested. The cross-sectional dimensions of the initial rectangular channel are 2.5 x 5.6 mm. By varying the type of heater foil material and its surface finish, the influence of these parameters on boiling can be assessed. If improved chemical inertness to other fluids is needed in future testing, the two polycarbonate plastic windows can be replaced with glass. Test-section flexibility will allow careful exploration of the parameters and mechanisms that influence small-channel boiling.

The video and optics used in this program furnish the high picture rates and magnification needed to achieve temporal and spatial resolution of nucleate-bubble growth and behavior in compact heat exchanger channels. Bubble growth is very fast in the initial stages after nucleation at a heated wall. The bubbles can be very small, occurring in channels a few mm or less in cross section.

The video camera is a Kodak SP2000 Motion Analysis System. The camera is monochrome and is based on a CCD sensor composed of a 240 x 192 pixel array. State-of-the-art data handling electronics allow full-frame video images to be taken at up to 2000 pps and viewed on a built-in 12-in. monitor. Additional selectable full-frame image rates are 60, 200, 500, and 1000 pps. By dividing the video image frame into 1/2, 1/3, or 1/6 segments, the system is capable of speeds of 4000, 6000, and 12000 pps, respectively. All images are recorded on Kodak 1/2-in. high-density magnetic tape in the form of a 1000-ft-long cassette tape. Tape playback is at 60 pps, with options of single frame or four slow-frame playbacks in forward or reverse. The system monitor also has an xy cursor with digital, on-screen readout of featured pixel locations. All recorded images can be digitized by system electronics and fed out in standard format to a computer for digital image analysis. The cassette is a nonstandard format but the system allows conversion to standard video format and transfer to an external recorder. The system is also capable of recording from two cameras simultaneously. Only one camera is available. The camera takes standard 35 mm C-mount lenses.

The lens used in this study is very important to the successful study of vapor bubble behavior. Because of the high frame-rates required and the light-acceptance inefficiencies of the camera CCD, the lens must have good light-gathering ability and must simultaneously furnish sufficient magnification with sufficient depth of field and field of view to allow imaging of the entire channel cross section. This must all be done at high magnification with good working distance between the lens and the image to be recorded. An Infinity Model K2 Long-Distance Microscope optics system was purchased. The lens has an effective aperture of 1.5 in. and furnishes variable working distances, magnification, and depth of field, depending on primary and eyepiece lenses, and on monitor size. With the purchased lenses and existing monitor, magnifications of up to 80x are achievable with fields of view and depth of field in the mm range. These capabilities are good for boiling channels of the size currently being tested. If smaller channels are studied, additional optics, which would allow magnifications as high as several hundred times, can be purchased. The current lens at highest magnification offers resolution of 189 lines/mm. This optics resolution is very adequate relative to the resolution of the CCD array and the actual requirement for seeing details of physical phenomena.

5 Summary

This report addresses results from the first phase of a program directed at obtaining an improved understanding of the physical mechanisms that influence boiling in compact heat exchangers. This is being done with high-speed video and microscope optics to characterize bubble nucleation, growth, and interaction within the confining walls of small heat transfer passages. Results from tests performed at ANL on boiling in small channels show that boiling behavior in small channels is different from that in large channels, with a nucleate-boiling mechanism dominating heat transfer to low values of wall superheat in small channels. Furthermore, there are no valid criteria available for designating a channel as large or small. Also, ANL scoping assessments of various mechanisms that may be responsible for the difference between the behavior in large versus small channels have shown that nucleate-bubble size (depending on fluid type, pressure, and thermal conditions) can become nominally the same as the channel cross section in channels 3 mm or less.

The evaluation of bubble size by various mechanistic bubble-diameter-prediction models emphasizes that the recent work by Zeng et al. (1993) on modeling bubble growth dynamics could be used to predict vapor bubble departure diameters better than the commonly used model of Firtz (1935). Hence, the model of Zeng et al. (1993) may be used in the first-stage development of an improved semimechanistic-based set of correlation parameters for nucleation-dominant flow-boiling in small channels. Paralleling the approach used by Rohsenow (1952), the Zeng et al. (1993) bubble model was used to define a set of nondimensional parameters that featured a new bubble Reynolds number based on vapor bubble dynamic growth forces rather than on surface tension, as in the work of Firtz (1935) and Rohsenow (1952). Initial efforts to use these parameters to correlate ANL small metal channel boiling data from nontransparent electrically heated test sections appear promising.

To establish information on actual bubble sizes in small channels and on the bubble/bubble and bubble/channel interactions, a test apparatus has been designed and built to utilize state-of-the-art ultra-high-speed-video-based flow visualization with microscope optics. This test apparatus will generate information that will allow establishment of criteria for designating when a boiling heat transfer channel is large or small; it will also allow development of a heat transfer correlation that has a specific correlation parameter that will reflect the influence of size scale on heat transfer along with the important Prandtl and bubble Reynolds numbers. The resulting more robust generalized correlations for heat transfer will allow greater confidence in the design of compact heat exchangers and reduce the need for tests to develop and verify performance.

Acknowledgments

This work was supported by the U.S. Department of Energy, Office of Energy Efficiency and Renewable Energy, Division of Advanced Industrial Concepts, and represents a U.S. contribution to the International Energy Agency (IEA) program on Research and Development in Heat Transfer and Heat Exchangers.

References

Carey, V. P., and Mandrusiak, G. D., 1986, "Annular Film-Flow Boiling of Liquids in a Partially Heated, Vertical Channel with Offset Strip Fins," Int. J. Heat Mass Transfer 29, 927-939.

Firtz, W., 1935, "Berechnung des Maximalvolumens von Dampfblasen," Physikalische Zeitschrift 36, 379.

Griffith, P., 1958, "Bubble Growth Rates In Boiling," ASME Trans. 80, 721-727.

Jakob, M., 1949, Heat Transfer, John Wiley and Sons, Inc., New York, Chapter 29.

Kasza, K. E., and Wambsganss, M. W., 1994, Unpublished information on boiling heat transfer in small channels, Argonne National Laboratory.

Kedzierski, M. A., and Kaul, M. P., 1993, "Horizontal Nucleate Flow Boiling Heat Transfer Coefficient Measurements and Visual Observations for R12, R134a, and R134a/Ester Lubricant Mixtures," 6th Intl. Symp. on Transport Phenomena (ISTP-6) In Thermal Engineering, Seoul, May 9-13, 1993.

Peng, X. F., and Wang, B.-X., 1993, "Forced Convection and Flow Boiling Heat Transfer for Liquid Flowing through Microchannels," Int. J. Heat Mass Transfer 36, 3421-3427.

Reay, D. A., 1988, "Impact of New Technologies on Future Heat Exchanger Design," Heat Recovery Systems and CHP 8, 309-314.

Robertson, J. M., 1979, "Boiling Heat Transfer with Liquid Nitrogen in Brazed-Aluminum Plate-Fin Heat Exchangers," Heat Transfer-San Diego 1979, AIChE Symposium Series 75(189), 151-164.

Robertson, J. M., 1983, "The Boiling Characteristics of Perforated Plate-Fin Channels with Liquid Nitrogen in Upflow," in Heat Exchangers for Two-Phase Applications, HTD-Vol 27, J. B. Kitto, Jr., and J. M. Robertson, eds., ASME, New York, 35-40.

Robertson, J. M., and Wadekar, V. V., 1988, "Vertical Upflow Boiling of Ethanol in a 10 mm Diameter Tube," Proc. 2nd UK National Heat Transfer Conference, Glasgow, Vol. 1, 67-77.

Rohsenow, W. M., 1952, "A Method of Correlating Heat-Transfer Data for Surface Boiling of Liquids," Trans. ASME 74, 969-975.

Shah, R. K., 1991, "Compact Heat Exchanger Technology and Applications," in Compact Heat Exchanger Technology: Current Practice and Future Developments, Inst. Chem. Eng., London, UK, 1-29.

Shah, R. K., and Robertson, J. M., 1993, "Energy Efficiency in Process Technology," in Compact Heat Exchangers For the Process Industry, P. A. Pilavachi, ed., Elsevier Applied Science, UK, 565-580.

Steiner, D., and Taborek, J., 1992, "Flow Boiling Heat Transfer in Vertical Tubes Correlated by an Asymptotic Model," Heat Transfer Eng. 13, 43-69.

Tran, T. N., Wambsganss, M. W., France, D. M., and Jendrzejczyk, J. A., 1993, "Boiling Heat Transfer in a Small, Horizontal, Rectangular Channel," Heat Transfer-Atlanta, AIChE Symp. Series 89(295), 253-261.

Vachon, R. I., Nix, G. H., and Tanger, G. E., 1968, "Evaluation of Constants for the Rohsenow Pool-Boiling Correlation," ASME J. Heat Transfer 90, 239-247.

Wadekar, V. V., 1992, "Flow Boiling of Heptane in a Plate-Fin Heat Exchanger Passage," in Compact Heat Exchangers for Power and Process Industries, HTD-Vol. 201, ASME, New York, 1-6.

Wambsganss, M. W., France, D. M., Jendrzejczyk, J. A., and Tran, T. N., 1993, "Boiling Heat Transfer in a Horizontal Small-Diameter Tube," Trans. ASME, J. Heat Transfer 115, 963-972; also, Argonne National Laboratory Report ANL-92/12, 1992.

Wambsganss, M. W., and Shah, R. K., 1994, "Vaporization in Compact Heat Exchangers," presented at Intl. Symp./Workshop on Boiling, Condensation, and Two-Phase Heat Transfer, Andhra University, Visakhapatnam, India, January 10-11, 1994.

Zeng, L. Z., Klausner, J. F., Bernhard, D. M., and Mei, R., 1993, "A Unified Model for the Prediction of Bubble Detachment Diameters in Boiling Systems-II. Flow Boiling," Int. J. Heat Mass Transfer 36, 2271-2279.

Zuber, N., 1961, "The Dynamics of Vapor Bubbles in Nonuniform Temperature Fields," Int. J. Heat Mass Transfer 2, 83-98.

Distribution for ANL–94/32

Internal

B. Arman
K. J. Bell
S. S. Chen
S. U. Choi
H. Drucker
D. M. France
J. A. Jendrzejczyk
K. E. Kasza (60)
C. A. Malefyt
T. J. Marciniak
N. T. Obot
C. B. Panchal
R. B. Poeppel
T. J. Rabas
N. F. Sather
W. W. Schertz
R. K. Smith
T. N. Tran
R. A. Valentin
M. W. Wambsganss (10)
R. W. Weeks
ANL Contract File
TIS Files

External

DOE-OSTI for distribution per UC-1423 (81)
ANL Libraries
    ANL-E (2)
    ANL-W
Manager, Chicago Field Office, DOE
Director, Technology Management Div., DOE-CH
D. L. Bray, DOE-CH
A. L. Taboas, DOE-CH
Energy Technology Division Review Committee:
    H. K. Birnbaum, University of Illinois, Urbana
    R. C. Buchanan, University of Cincinnati, Cincinnati, OH
    M. S. Dresselhaus, Massachusetts Institute of Technology, Cambridge, MA
    B. G. Jones, University of Illinois, Urbana
    C.-Y. Li, Cornell University, Ithaca, NY
    S.-N. Liu, Fremont, CA
    R. E. Smith, SciTech, Inc., Morrisville, NC